Data Repository item 2004173

GSA Repository Part A. (Quade et al. Paleoenvironments of the Earliest Toolmakers (B25358).

Type sections of the Busidima Formation, Gona, NE Ethiopia.

Our intent here is to establish the type sections for the Busidima Formation. The entire Busidima Formation is not exposed continuously in any one location. So we have selected three measured sections that encompass most or all of the known Busidima Formation thickness (Fig. 1 repository). Section EG99-001 (Fig. 2a) is located on the NE bank of the Kada Gona River and passes through the classic Oldowan archeological sites described in Semaw et al. (1997). This spans most of what we would informally call the lower Busidima Formation. The upper Busidima Formation is covered by section BUS03-12/13 (Fig. 2b) on the north side of the Busidima River, and section AS03-04 (Fig. 2c) south of the Busidima. We currently estimate the lower Busidima Formation to span the period 2.7 to 1.6 Ma, and the upper Busidima Formation 1.6 to 0.5 Ma.

Lithofacies designations used in Figures 2a-c are the same as those described in the main text of the article. The numbers 1 and 2 appended to each lithofacies denote Type I (paleo-Awash) and Type II (paleo-Awash tributary) associations (see text).

Gravel dominated (G)

Gt: conglomerate with trough cross-beds

Gm: massive conglomerate

Gms: massive conglomerate with sandy matrix

Sand dominated (S):

St: sandstone with trough cross-beds

Sm: massive sandstone

Sr: sandstone with ripples

Mud dominated (F):

Fh: horizontally bedded mudstone

Fm: massive mudstone

Fp: pedogenically altered mudstone

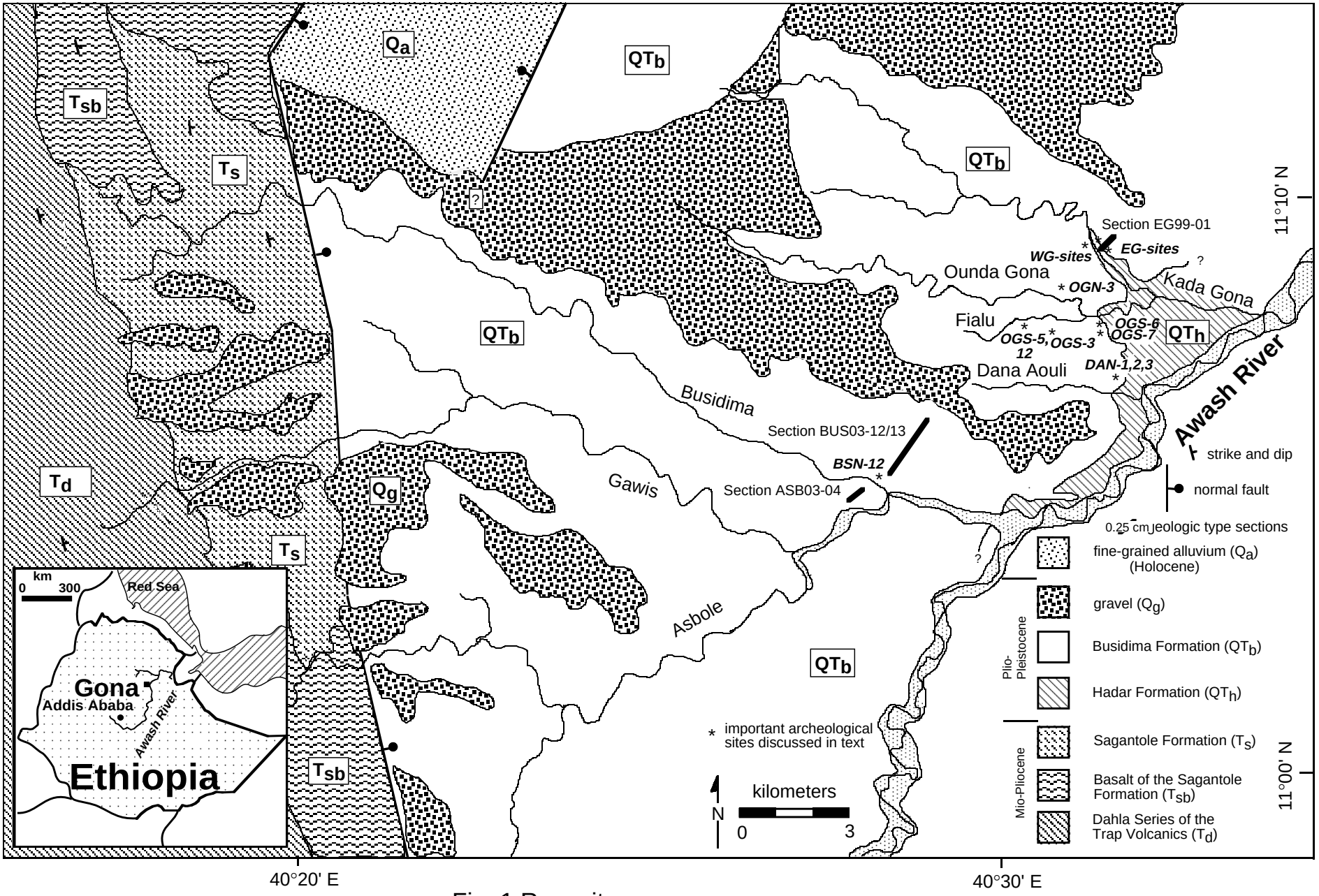

Fig. 1 Repository

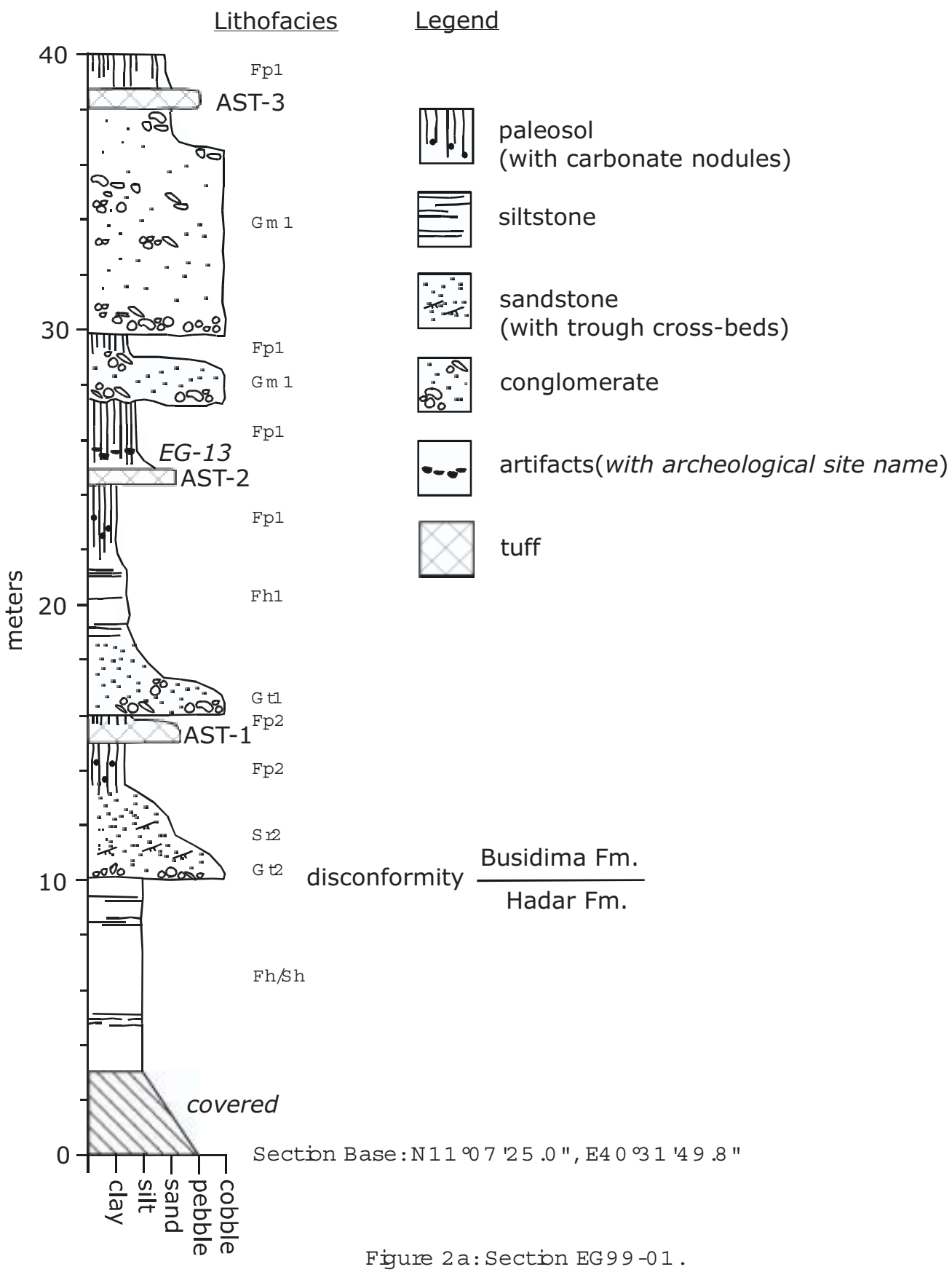

Figure 2a: Section EG99-01.

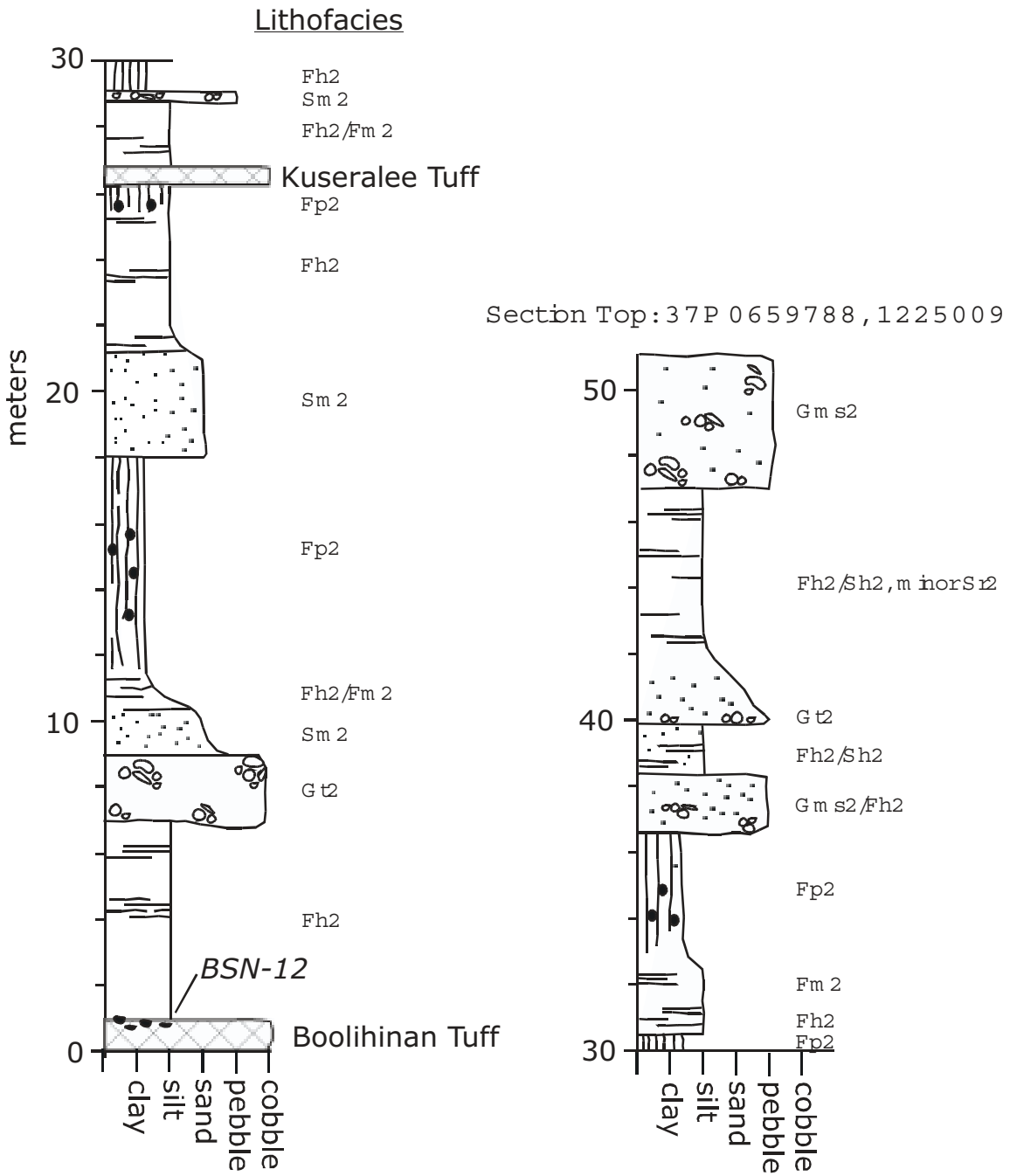

Figure 2b: Section BUS99-12/13. See Fig. 2a for legend.

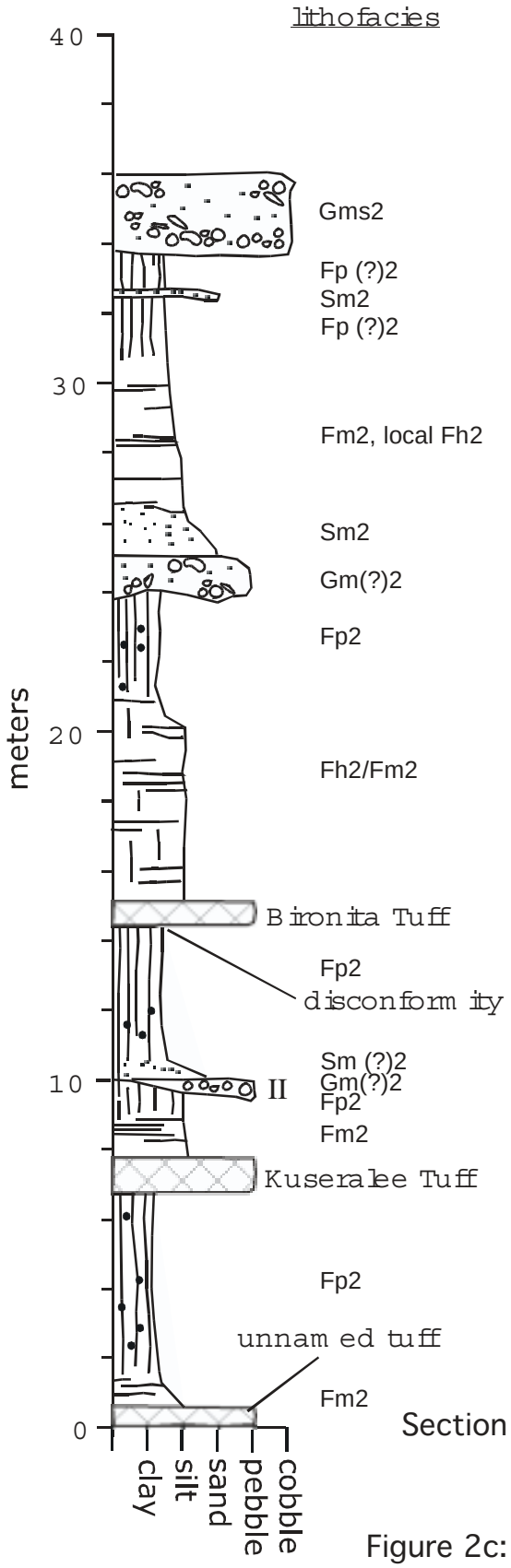

Section Base: 37P 0658341, 1224558

Figure 2c: Section ASB03-04. See Fig.2a for legend.

GSA Repository Part B. (Quade et al. Paleoenvironments of the Earliest Toolmakers (B25358).

Procedure for estimation of %C_4 biomass and associated error:

Fraction C_4 biomass = $(\iota\,^{13}C_{sc}-\iota\,^{13}C_{C3})/(\iota\,^{13}C_{C4}-\iota\,^{13}C_{C3})$ (1)

where:

$\iota\,^{13}C_{sc}$ = the carbon isotopic value for soil carbonate

#

$\iota\,^{13}C_{C3}$ = the average carbon isotopic value for soil carbonate formed in equilibrium with East African C_3 vegetation.

#

$\iota\,^{13}C_{C4}$ = the average carbon isotopic value for soil carbonate formed in the presence of East African C_4 vegetation.

All errors are assumed to be indeterminant and are stated at ±1ω throughout. Error propogation procedures follow those described in Bevington and Robinson (2002) and in Skoog and West (1982).

Equation (1) requires that we estimate the values of $\iota\,^{13}C_{C3}$ and $\iota\,^{13}C_{C4}$ and their associated errors. To do this we will (1) first obtain $\iota\,^{13}C$ averages for East African C_3 and C_4 plants, and then (2) translate these into $\iota\,^{13}C$ values for coexisting soil carbonate, (3) apply this estimate and its associated errors to equation (1)

/80#t ^{13}C values are not available for modern Ethiopian C_3 and C_4 plants, but they are available from other areas of East Africa to the south, mainly Uganda and Kenya. We drew upon the recent compilation of $\iota\,^{13}C$ values from Cerling and others (2003) for a variety settings (Table 1). We selected values from areas such as open canopy forest, savanna, and bushland most analogous to Ethiopia today and probably throughout much of the Neogene (based on pollen evidence from Bonnefille and others, 1987).

Table 1. Compilation of ι ^{13}C values for East African Plants (data from Cerling and others, 2003)

setting	**pathway**	**ι ^{13}C (mean)**	**±1s**	**N (plants)**	
Open-canopy forest, bushland	C_3 dicots	-27.02	1.28	137	
xeric bushland and savanna, and open canopy forest	C_4	-13.27	1.42	105	mostly NAD, PCK C_4 metabolic pathways

(2a) the isotope enrichment factor (κ) (in ‰) between $CaCO_3$ and CO_2 (from Romanek and others, 1992) for ^{13}C and ^{12}C is related to temperature T as:

κ#$CaCO_3$-CO_2) = 11.98 (±0.13)-0.12(±0.01) x T (°C) (2)

If mean annual temperature at Gona is 26°C today, and was 5°C colder during glacial periods (probably an upper bound for this low latitude at 9°N, then we can use 23.5±2.5°C as safely encompassing soil temperature fluctuations at> 50 cm over the past 3 Ma. Use of this temperature range and the uncertainties in the fractionation equation yield an enrichment factor for this step of 9.16±0.17. The small uncertainty reflects the relative insensitivity of κ#$CaCO_3$-CO_2) for ^{13}C and ^{12}C as compared to, for example, κ#$CaCO_3$-CO_2) for ^{18}O and ^{16}O.

(2b) we use a kinetic enrichment of 4.4‰ in ^{13}C, resulting from diffusive transfer of soil CO_2. This value is calculated from the differing diffusion rates of $^{13}CO_2$ and $^{12}CO_2$ in air, represented as:

$Ds^{12}CO_2 / Ds^{12}CO_2 = [((m_{air} + m^{12}CO_2)/(m_{air} \times m^{12}CO_2)) \times ((m_{air} \times m^{13}CO_2)/(m_{air} + m^{13}CO_2))]^{1/2} = 1.0044$

Where:

$Ds^{12}CO_2$: diffusion coefficient of $^{12}CO_2$ in air
$Ds^{12}CO_2$: diffusion coefficient of $^{13}CO_2$ in air
m_{air} =mass of air
$m^{12}CO_2$ = mass of $^{12}CO_2$

$m^{13}CO_2$ = mass of $^{13}CO_2$

Error in this calculation depends on the errors in the mass estimates of air, and $^{13}CO_2$ and $^{12}CO_2$, errors which are considered to be negligible. Diffusion coefficients are not temperature dependant, so there is no error associated with uncertainty in soil air temperatures. The ~4.4‰ enrichment between the $\iota^{13}C$ value of soil CO_2 (concentrations) and soil-respired CO_2 (flux) is also observed in direct soil measurements (Cerling and others, 1991).

(2c) we assume simple mixing of CO_2 from C_3 and C_4 plants, since respiration rates past and present (see text) should have been high enough to exclude atmospheric CO_2.

(2d) the $\iota^{13}C$ values of atmospheric CO_2 has increased in the last 150 years due fossil fuel burning (the Suess Effect) atmosphere. We must correct for this in order to use the $\iota^{13}C$ values of modern plants as a basis for interpreting the $\iota^{13}C$ value of ancient soil carbonates. This value is estimated to be 1.48±0.1 since 1850 (Friedli and others, 1986), and we adopt this estimate for the deeper geologic past.

Combining the diffusion and Suess Effects with the equilibrium fractionation factor (equation 2) gives an enrichment estimate of 15.0±0.2‰ between coexisting soil carbonate and plant-derived soil CO_2.

(2e) Combining this enrichment factor in 2c with our the calculated averages of $\iota^{13}C$ values for C_4 and C_3 plants in East Africa from (1) gives:

$\iota^{13}C_{C4} = +1.8 \pm 1.4$

$\iota^{13}C_{C4} = -12.0 \pm 1.3$

#

These values can be plugged into equation (1), and errors estimated for a range of $\iota^{13}C_{sc}$ values encompassing the values seen at Gona. The ±1s for the fraction C_4 biomass comes out at 0.17 or ±17%.

(3) Finally, calculation of $\%C_4$ from individual $\iota^{13}C$ values of soil carbonates requires that we propagate the laboratory error in our laboratory in reproducing the accepted $\iota^{13}C$ value of the Carrera Marble Standard. This subsumes analytical error, and any random error arising from (1) inhomogeneities in our lab standard and from (2) the extraction procedure . The long-term standard deviation for these standard measurements for my lab is ±0.09‰. Incorporation of this error in the cumulative ±17% error from (2e) is negligible.

References (for GSA Repository Part B)

Bevington, P. R. and Robinson, D. K., 2002, Data Reduction and Analysis for the Physical Sciences. 3rd Edition. MacGraw Hill, 320p.

Bonnefille, R., Vincens, A., and Buchet, G., 1987, Palynology, stratigraphy and palaeoenvironment of a Pliocene hominid site (2.9-3.3 M.Y.) at Hadar, Ethiopia: Palaeogeography, Palaeoclimatology, Palaeoecology, v. 60, p. 249-281.

Cerling, T. E., Solomon, D. K., Quade, J., and Bowman, J. R., 1991, On the isotopic composition of carbon in soil carbon dioxide: Geochimica et Cosmochimica Acta, v. 55, p. 3403-3405.

Cerling, T. E., Harris, J. M., and Passey, B. H., 2003, Diets of East African Bovidae based on stable isotope analysis. Journal of Mammalogy, v. 84 (2), p. 456-470.

Diffusion equation

Freidli, H., Lotscher, H., Oeshger, H., Siegenthaler, U., and Stauffer, B., 1986, Ice core record of 13C/12C ratio of atmospheric CO2 in the past two centuries: Nature, v. 324, p. 237-238.

Romanek, C. S., Grossman, E. T., and Morse, J. W. (1992). Carbon isotopic fractionation in synthetic aragonite and calcite: effects of temperature and precipitation rate: Geochimica et Cosmochimica Acta, v. 56, p. 419-430.

Skoog, D. A. and West, D. M., 1982, Fundamentals of Analytical Chemistry. Saunders Pub. Co., New York, 4th edition. 804p.

OXYGEN ISOTOPIC RESULTS FROM GONA

sample number	sample type*	feature	age (Ma)	$\iota^{18}O$ (PDB)
Busidima Formation				
DANL 10	gravel coating		0.3	-4.58
DANL 19	gravel coating		0.3	-4.39
GONJQ253	gravel coating		0.3	-5.02
GONJQ144	gravel coating		0.3	-6.38
GONJQ 62	gravel coating		0.3	-4.68
DANL-101	gravel coating		0.3	-3.59
GONJQ 6a	gravel coating		0.3	-2.52
GONJQ 6b	gravel coating		0.3	-3.59
GONJQ 5a	nodule		1.1	-6.59
GONJQ 83a	nodule		1.3	-6.52
GONJQ 3a	nodule		1.3	-4.80
GONJQ 77a	nodule		1.35	-6.33
GONJQ 78a	nodule		1.35	-9.53
GONJQ 79a	contact nodule		1.35	-7.91
GONJQ 80a	reworked nodule		1.35	-6.90
GONJQ 84a	nodule		1.35	-5.90
GONJQ 2a	nodule		1.35	-5.67
GONJQ112a	nodule		1.4	-5.43
GONJQ109a	S1 rhizolith		1.5	-5.71
GONJQ 73a	nodule		1.5	-6.15
GONJQ 66a	nodule		1.6	-5.75
GONJQ 86a	platey	paleosol profile A	1.8	-6.64
GONJQ 86b	platey	paleosol profile A	1.8	-6.98
GONJQ 87b	soil rhizolith	paleosol profile A	1.8	-5.59
GONJQ 88a	platey	paleosol profile A	1.8	-6.48
GONJQ 88b	platey	paleosol profile A	1.8	-6.00
GONJQ 89a	nodule	paleosol profile A	1.8	-7.63
GONJQ 90a	platey	paleosol profile B	1.8	-5.07
GONJQ 91a	nodule	paleosol profile B	1.8	-5.75
GONJQ 92a	nodule	paleosol profile B	1.8	-4.36
GONJQ 93a	nodule	paleosol profile B	1.8	-4.63
GONJQ 63a	nodule		2	-6.30
GONJQ 95a	nodule	paleosol profile C	2	-6.37
GONJQ 95b	nodule	paleosol profile C	2	-6.26
GONJQ 95c	nodule	paleosol profile C	2	-6.43

GONJQ 96a	soil rhizolith	paleosol profile C	2	-5.95
GONJQ 96b	soil rhizolith	paleosol profile C	2	-6.34
GONJQ 97a	platey	paleosol profile C	2	-5.35
GONJQ 97b	platey	paleosol profile C	2	-10.83
GONJQ 97c	platey	paleosol profile C	2	-5.63
GONJQ 99A1	nodule		2	-6.08
GONJQ 99A2	nodule		2	-6.02
GONJQ 99A3	nodule		2	-6.05
GONJQ 99A4	nodule		2	-6.03
GONJQ 13a	nodule		2.2	-6.36
GONJQ 47a	nodule		2.55	-6.41
GonJQ100a	nodule		2.55	-7.33
GONJQ101a	nodule		2.55	-6.27
GONJQ 10a	nodule		2.55	-7.36
GONJQ 11a	platey		2.55	-6.68
GONJQ 46a	S1 rhizolith		2.6	-6.57
GONJQ 59a	nodule		2.6	-3.26
GONJQ 7a	nodule		2.6	-6.90
GONJQ 8a	soil rhizolith		2.6	-6.54
GONJQ 9a	nodule		2.6	-6.57
Hadar Formation				
GONJQ 52a	platey		2.9	-5.54
GonJQ 19a	nodule		2.95	-7.17
GONJQ 17A1	nodule	nodule A	3.15	-5.53
GONJQ 17A10	nodule	nodule A	3.15	-5.48
GONJQ 17A2	nodule	nodule A	3.15	-6.16
GONJQ 17A3	nodule	nodule A	3.15	-5.91
GONJQ 17A4	nodule	nodule A	3.15	-6.11
GONJQ 17A5	nodule	nodule A	3.15	-5.25
GONJQ 17A7	nodule	nodule A	3.15	-5.30
GONJQ 17A9	nodule	nodule A	3.15	-6.38
GONJQ 17b1	nodule	nodule B	3.15	-5.68
GONJQ 51a	nodule		3.16	-3.90
GONJQ 21a	nodule		3.17	-7.40
GONJQ 27a	nodule		3.19	-5.68
GONJQ 38a	nodule		3.2	-8.06
GONJQ 49a	nodule		3.2	-6.96
GONJQ 36a	nodule		3.24	-5.79
GONJQ 25a	nodule		3.25	-5.25
GONJQ 26a	nodule		3.25	-5.57
GONJQ 23a	nodule		3.26	-7.55
GONJQ 40a	nodule		3.26	-4.68
GONJQ 31a	nodule		3.31	-9.70